Accepted Manuscript

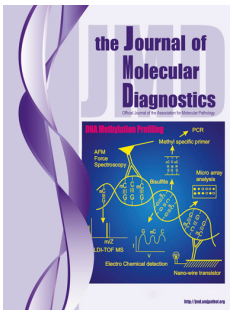

Structural Variation Detection by Proximity Ligation from Formalin-Fixed, Paraffin-Embedded Tumor Tissue

Christopher J. Troll, Nicholas H. Putnam, Paul D. Hartley, Brandon Rice, Marco Blanchette, Sameed Siddiqui, Javkhlan-Ochir Ganbat, Martin P. Powers, Ramesh Ramakrishnan, Christian A. Kunder, Carlos D. Bustamante, James L. Zehnder, Richard E. Green, Helio A. Costa

PII: S1525-1578(18)30172-7

DOI: https://doi.org/10.1016/j.jmoldx.2018.11.003

Reference: JMDI 761

To appear in: *The Journal of Molecular Diagnostics*

Received Date: 20 April 2018

Revised Date: 23 October 2018

Accepted Date: 17 November 2018

Please cite this article as: Troll CJ, Putnam NH, Hartley PD, Rice B, Blanchette M, Siddiqui S, Ganbat J-O, Powers MP, Ramakrishnan R, Kunder CA, Bustamante CD, Zehnder JL, Green RE, Costa HA, Structural Variation Detection by Proximity Ligation from Formalin-Fixed, Paraffin-Embedded Tumor Tissue, *The Journal of Molecular Diagnostics* (2019), doi: https://doi.org/10.1016/j.jmoldx.2018.11.003.

Structural variation detection by proximity ligation from formalin-fixed, paraffin-embedded tumor tissue

Christopher J. Troll,* Nicholas H. Putnam,* Paul D. Hartley,* Brandon Rice,* Marco Blanchette,* Sameed Siddiqui,* Javkhlan-Ochir Ganbat,* Martin P. Powers,* Ramesh Ramakrishnan,* Christian A. Kunder,† Carlos D. Bustamante,‡ § James L. Zehnder,† Richard E. Green,¶ and Helio A. Costa†‡

From Dovetail Genomics, LLC,* Santa Cruz; the Departments of Pathology,† Biomedical Data Science,‡ and Genetics,§ Stanford University School of Medicine, Stanford; and the Department of Biomolecular Engineering, University of California Santa Cruz, Santa Cruz, California

Correspondence to: Richard E. Green, Ph.D., UC Santa Cruz, Department of Biomolecular Engineering, 1156 High St, Biomed 146, Santa Cruz, CA 95064. Email: ed@soe.ucsc.edu; or Helio A. Costa, Ph.D., Stanford University, Department of Pathology, 300 Pasteur Drive, MSOB x313, Stanford, CA 94305. Email: hcosta@stanford.edu.

Short Title: FFPE fusion detection by proximity ligation.

Disclosure: This research was funded by Dovetail Genomics, LLC. C.D.B. is on the scientific advisory boards (SAB) of AncestryDNA, Arc Bio LLC, Etalon DX, Liberty Biosecurity, and Personalis. C.D.B. is on the board of EdenRoc Sciences LLC. C.D.B. is also a founder and SAB chair of ARCBio. None of these entities played a role in the design, execution, interpretation, or presentation of this study. C.T., N.P., P.D.H, B.R., M.B., S.S., J.G., and M.P.P. are employees of Dovetail Genomics, LLC. R.E.G is the founder of Dovetail Genomics. C.T., N.P., P.D.H., M.B. and M.P.P. have applied for patents related to this study.

Abstract

The clinical management and therapy of many solid tumor malignancies is dependent on detection of medically actionable or diagnostically relevant genetic variation. However, a principal challenge for genetic assays from tumors is the fragmented and chemically damaged state of DNA in formalin-fixed, paraffin-embedded (FFPE) samples. From highly fragmented DNA and RNA there is no current technology for generating long-range DNA sequence data as is required to detect genomic structural variation or long-range genotype phasing. We have developed a high-throughput chromosome conformation capture approach for FFPE samples that we call “Fix-C”, which is similar in concept to Hi-C. Fix-C enables structural variation detection from archival FFPE samples. This method was applied to 15 clinical adenocarcinoma and sarcoma positive control specimens spanning a broad range of tumor purities. In this panel, Fix-C analysis achieves a 90% concordance rate with FISH assays - the current clinical gold standard. Additionally, novel structural variation undetected by other methods could be identified and long-range chromatin configuration information recovered from these FFPE samples harboring highly degraded DNA. This powerful approach will enable detailed resolution of global genome rearrangement events during cancer progression from FFPE material and inform the development of targeted molecular diagnostic assays for patient care.

Introduction

A major hurdle in developing genomic tools for detection of medically actionable genetic variation in cancer is that in clinical practice solid tumor tissue commonly undergoes formalin-fixed paraffin-embedded (FFPE) processing for both pathological cancer diagnosis and exploratory histology–based cancer research projects[1]. This common procedure for pathology samples serves a crucial function, allowing tumor diagnosis and classification via several established procedures. However, the formalin fixation process induces chemical modifications by cross-linking nucleic acids and protein. The result of this is that DNA and RNA become fragmented[2,3]. Thus, technologies using long DNA segments for variant detection perform poorly with FFPE nucleic acid.

The current gold-standard assay for structural variation using FFPE samples is fluorescence *in situ* hybridization (FISH). However, FISH is limited to well characterized fusion breakpoint regions. Unknown fusion breakpoint sites, even of clinically actionable gene-pairs, result in false negative diagnostic results and can lead to downstream complications due to improper treatment or require additional orthogonal testing. Alternative genomic approaches using DNA next-generation sequencing have been developed to efficiently detect gene fusions in a clinical cancer setting[4]. Although this allows higher throughput fusion detection, targeted DNA panels commonly used in cancer profiling still only capture a small range of the potential genomic breakpoint regions and are entirely dependent on a low number of fusion ‘spanning’ or fusion ‘straddling’ reads for detection support. Since repetitive or low complexity DNA sequences often mediate genome rearrangements[5], traditional short-read sequencing is often unable to unambiguously span these breakpoints. RNA sequencing methods can identify rearrangements in a high-throughput manner but are limited to fusions occurring in the coding

regions of sufficiently expressed transcripts, potentially missing lowly expressed fusions as well as intronic and intragenic rearrangements.

Proximity ligation protocols, such as Hi-C, are techniques that characterize the spatial organization of chromatin in a cell[6]. These techniques work by using formaldehyde to create crosslinks between histones and other DNA-associated proteins to stabilize the three-dimensional organization of chromatin in living cells. The chemical cross-links stabilize chromatin through subsequent molecular biology steps. In Hi-C, these steps include cutting the DNA with a restriction enzyme, marking the free ends with biotin during a fill-in reaction, and ligating the blunt ends with ligase. The ligation products, in many cases, are then chimeric products between segments of the genome that are in close physical proximity, but not necessarily adjacent in linear sequence. Proximity ligation DNA products are captured in bulk using streptavidin. High throughput read pair sequencing of proximity ligation libraries generates a genome-wide census describing which genomic regions are proximal to which other regions.

Although Hi-C was developed to probe the three-dimensional architecture of chromosomes in living cells, it has also been used off-label for genome scaffolding[7-9]. The key insight is that most proximity ligation products are in close physical proximity because they are in linear proximity along the genome. In fact, the probability of a given distance between ligated segments is well described by a power law function as would be expected from the polymer nature of DNA. This regular property of proximity ligation data is the basis for its use in applications other than probing the three-dimensional architecture of genomes in cells. For example, genome scaffolding is possible from proximity ligation data by mapping read pairs to genome contigs. Because proximity-ligation read pairs only derive from linked, ie, same chromosome segments, it is possible to assign contigs to their linkage groups. Furthermore,

closely linked contigs will generate more proximity ligation products than contigs that are spaced further in the genome. This property is exploited to order and orient contigs.

Additionally, proximity ligation data can be used to detect and phase structural variants. In this approach, proximity ligation data are compared to what would be expected in a reference genome by mapping reads against a known reference. If the sample in question has a genome rearrangement or other structural variation, a population of read pair density it will appear where none is expected. For example, a chromosomal translocation will result in read pairs that map to the regions of the two chromosomes that have fused. Ordinarily none or few such chimeric proximity ligation products are expected.

Materials and Methods

Specimens and nucleic acid extraction

The patient tissue specimens described in this study were obtained from formalin-fixed, paraffin-embedded (FFPE) tissue blocks from the Stanford Cancer Center under institutional review board (IRB)-approved protocols. An anatomical pathologist reviewed, diagnosed, and estimated tumor purity from hematoxylin and eosin (H&E) slides of each specimen. A non-tumor normal FFPE spleen tissue block (BioChain Paraffin Tissue Section, Cat. No. T2234246) was used as a control for the Fix-C analysis. Somatic RNA for traditional RNAseq from patient and control samples were extracted using a Qiagen RNeasy FFPE Kit (Qiagen Inc., Germantown, MD), respectively. Specimen age, tissue volume, and origin of the tissue can be found in **Supplemental Table S1**.

Somatic DNA for Fix-C analysis was extracted by incubating a 10 µm scroll of FFPE tissue with 1 mL of xylene (Sigma, #534056) in a 1.5 mL microcentrifuge tube (LoBind,

Eppendorf, #022431021), centrifuging one minute at 13.2 x g, aspirating the supernatant, resuspending the pellet with 1 mL of 100% ethanol, centrifuging one minute at 13.2 x g, and opening the microcentrifuge tubes to allow the ethanol to evaporate at room temperature. A solution of 50mM Tris-HCl (pH8.0), 1% SDS, 0.25mM $CaCl_2$, and 0.5mg/mL proteinase K was then added to each sample and incubated at 37 °C for one hour. After incubation, the samples were centrifuged for 1 minute at 13.2 x g. The supernatant from each tube was transferred to a new 1.5 mL microcentrifuge tube (LoBind, Eppendorf, #022431021). One molar NaCL and 18% PEG-8000 were added to 1 mL para-magnetic carboxylated beads (GE, #65152105050250). One-hundred microliter of the suspended para-magnetic bead solution was added to the sample microcentrifuge tube and incubated 10 minutes. After concentrating the beads on a magnetic rack, the beads were washed twice with a solution of 50mM NaCl 10mM Tris-HCl (pH8.0). The solid-substrate bound chromatin was digested by suspending the carboxylated beads in 50uL of 1x cutsmart buffer (NEB B7204S) and 10U/uL MboI (NEB R0147L) for one hour at 37 °C. After restriction enzyme digestion, the beads were concentrated on a magnetic rack and washed twice with a solution of 50mM NaCl and 10mM Tris-HCl (pH8.0). The beads were then suspended in 50uL of 1x buffer 2 (NEB B7002S) combined with 150uM dGTP, dTTP, dATP, and 40uM biotintylated dCTP and 5U/uL of klenow large fragment (NEB M0210L) and incubated at 25 °C for 30 minutes. The beads were then concentrated on a magnetic rack and washed twice with a solution of 50mM NaCl 10mM Tris-HCl (pH8.0). The beads were then suspended in 250uL of 1x T4 ligase buffer (NEB B0202S) and 2,000U/uL T4 ligase (NEB M0202M) and incubated for one hour at 16 °C. Next, the beads were concentrated on a magnetic rack and the supernatant was removed. A solution of 50mM Tris-HCl (pH8.0), 1% SDS, 0.25mM $CaCl_2$, and 0.5mg/mL proteinase K was added to each tube and the samples were

incubated at 55 °C for 15 minutes and then 68 °C for 45 minutes. Lastly, the beads were concentrated on a magnetic rack and the supernatant was placed into a new tube. Fix-C DNA was purified from the supernatant using Agencourt AMPure XP beads (Beckman Coulter A63882) and quantified using a Qubit fluorometer.

Fix-C sample preparation, sequencing, and fusion detection

Fix-C DNA was sheared to between 200 to 500 base-pairs using a Diagenode Bioruptor Pico at seven cycles of shearing with 15 seconds on and 90 seconds off. After shearing, Fix-C DNA was put through end repair and A-tailing, as well as next-generation sequencing adapter ligation using the NEB Ultra II DNA Library Prep Kit for Illumina (E7645L). After adapter ligation, Fix-C DNA was bound to 20uL of MyOne Streptavidin C1 Dynabeads suspended in 10mM Tris-HCl (pH8.0), 2M NaCl, and 0.5mM EDTA for 30 minutes at room temperature. After C1 bead enrichment, the beads were magnetically concentrated and then washed twice with 10mM Tris-HCl (pH8.0), 1M NaCl, 1mM EDTA, and 0.05% Tween-20, and then twice with 50mM NaCl 10mM Tris-HCl (pH8.0). Beads were then placed in an Index PCR reaction with Kapa HiFi Hotstart ReadyMix (KK2602), using the supplied NEB universal primer and an appropriate index primer and incubated in a thermocycler using specifications defined by Kapa HiFi. After index PCR, Fix-C DNA was purified using a 0.8x Ampure purification protocol. Fix-C DNA concentration, molarity, and size was then quantified via Qubit fluorometry and Agilent High Sensitivity D1000 Tape and an associated Tapestation. For quality control and genotype inferences, reads were aligned to the human reference sequence GRCh38 using a modified version of the SNAP aligner[10], as previously described[9]. For quality control of Fix-C DNA in terms of expected PCR duplication rate, estimated library complexity, and intra-aggregation

insert distribution, libraries were spiked in at 5% each on a 2x76 PE MiSeq run. For gene fusion identification libraries were sequenced to adequate depth on a high throughput Illumina sequencer as informed by the estimated library complexity from the MiSeq QC. Most libraries were sequenced between 150 and 250 million read pairs. Dovetail modified SNAP aligner was used on paired end sequence with following parameters: snap paired <REF_INDEX_DIR> <READ1> <READ2> -xf 3.0 –t32 –o –bam <BAM_OUTPUT> -ku –as –C-+ -tj GATCGATC –mrl 20 –pf <SNAP_STAT_LOG_OUTPUT>. Read pairs mapping between annotated segmental duplications in the human genome were removed[11]. Chromosomal rearrangements and gene fusions were assessed by dividing the reference genome into non-overlapping bins of width *w*, and tabulating N_{ij} the number of read pairs which map with high confidence (MAPQ > 20) to bins *i* and *j*, respectively. To automatically identify genomic rearrangement junctions, a statistic that identifies local contrasts in N_{ij} characteristic of rearrangements was defined. Assuming Poisson-distributed local read counts, two z-scores were computed at each bin

$$i,j : Z^{+}_{ij}=(N^{+}_{ij}.-N^{-}_{ij})/\sqrt{N^{-}_{ij.}} \text{ and } Z^{-}_{ij}=(N^{-}_{ij}.-N^{+}_{ij})/\sqrt{N^{+}_{ij.}}$$

Where N^{+}_{ij} is the local sum over north-east and south-west quadrants of N_{ij} up to a maximum range

$$\text{R: } N_{ij}^{+} = \sum_{k=i,l=j}^{k=i+R,j+R} N_{kl} + \sum_{k=i,l=j}^{k=i-R,j-R} N_{kl},$$

and N^{-}_{ij} is a similar sum over north-west and south-east quadrants:

$$N_{ij}^{-} = \sum_{k=i,l=j}^{k=i-R,j+R} N_{kl} + \sum_{k=i,l=j}^{k=i+R,j-R} N_{kl}.$$

All positions *ij* for which

$$\max(Z^{+}_{ij}, Z^{-}_{ij}) > Z_{min}=10 \text{ and } \max(Z^{+}_{ij}, Z^{-}_{ij})$$

is a local maximum (no positions i,j have a higher value within a range of 3w) were defined as candidate fusion junctions. In this way, the N_{ij}^{+} statistic measures provides the signal for evidence of a rearrangement and the N^{-}_{ij} statistic provides the signal for the local background of proximity ligation data in the regions under scrutiny. Importantly, this local normalization minimizes the combined effects of local variations in mappability, GC%, density of restriction sites, etc. This simple normalization works by measuring the observed rate, genome-wide, of read-pairs mapping in each bin which can be higher or lower than expected for a wide variety of biological or technical reasons, all subsumed by this normalization. This approach will minimize false positive calls. However, genomic regions that fail to generate proximity ligation data altogether may fail in this approach. Thus, false negatives are possible. After identifying candidate fusions at an initial bin size w_0 = 50000, breakpoint position was refined by re-applying the same criteria to a local region surrounding each candidate with successively smaller values of w: 10000 and 5000.

RNA sequencing sample preparation, sequencing, and fusion detection

Total RNA from each specimen underwent enrichment for a 44-gene targeted RNA fusion panel using Nimblegen SeqCap target enrichment probes (Roche Sequencing, Pleasanton, CA).

Sequencing libraries were then constructed and sequenced on an Illumina MiSeq instrument producing 100bp paired end reads. In brief, sequencing reads were mapped to the human reference genome (hg19) using the FusionCatcher algorithm (v 0.99.7) which uses a meta-aligner approach with STAR, BOWTIE2, and BLAT to align reads and then subsequently detects fusion transcripts using the following parameters: fusioncatcher/bin/fusioncatcher -i <R1.fastq.gz>,<R2.fastq.gz> -o <output folder> -d ensembl_v84 -z -p 14 --visualization-sam --visualization-psl. Called variants were annotated for a series of functional predictions, conservation scores, in addition to publicly available database annotations using a combination of perl scripts and ANNOVAR[12](12).

Fluorescent *In Situ* Hybridization (FISH)

FISH analysis was performed on interphase nuclei or metaphase chromosomes with the corresponding break-apart FISH probe (Empire Genomics, Buffalo, NY) as previously described[13](13). Microscopic analysis and imaging was performed with an Olympus BX51 microscope equipped with an 100x oil immersion objective, appropriate fluorescence filters and CytoVision® imaging software (LeicaBiosystems, Buffalo Grove, IL).

Statistical analyses

All statistical analyses were performed in the R programming language.

Results

We hypothesized that the first step of FFPE sample processing, ie, formaldehyde fixation, may render samples with the spatial organization of chromatin intact, regardless of the unwanted

effects of FFPE processing, including DNA fragmentation (**Figure 1A**). High molecular weight DNA was extracted from several FFPE samples. In each case, the DNA was no longer than a few tens of kilobases and generally less than one kilobase (**Figure 1B**). Notably, the DNA recovered from several samples had visible banding at mono-, di-, and tri-nucleosome sizes indicating that DNA fragmentation likely occurs on intact chromatin. Due to the short size of DNA in FFPE samples, genetic assays including long-read sequencing or barcoding that requires intact, high molecular weight DNA are not possible from FFPE samples.

To test the hypothesis that FFPE samples retain long-range genomic information, a custom proximity ligation protocol was designed for FFPE samples. This protocol includes the central steps of Hi-C (**Figure 1A**) but is preceded by solubilizing the chromatin from FFPE samples under mild proteolytic conditions that are meant to retain the cross-linked DNA-histone complexes prior to performing enzymatic digestion. Following digestion, the digested DNA fragments are biotinylated—serving as a marker for subsequent enrichment. The biotinylated DNA fragments are subsequently re-ligated in conditions that promote ligation of neighboring DNA chromatin fragments in close physical proximity. Thus, proximity ligation generates segments of DNA, marked with biotin, that are chimeras of two genomic segments that happened to be in close physical proximity in chromatin. Following crosslink reversal, DNA shearing, and biotin capture on streptavidin beads, standard Hi-C–like high-throughput sequencing libraries were generated and the proximity of the ligated DNA measured by high-throughput paired-end DNA sequencing[14].

Complex Fix-C libraries were created with a high percent of reads capturing long-range contacts using as little material as one 10um FFPE scroll. However, FFPE samples were highly variable with respect to DNA yield. The Fix-C protocol is designed to retain chromatin-

associated DNA while discarding naked DNA. The amount of proximity-ligated DNA recovered from the Fix-C protocol is typically in the tens of nanograms whereas total DNA extracted from FFPE scrolls is generally an order of magnitude higher.

Paired-end sequences of these Fix-C libraries were mapped to the reference human genome to assess library complexity and to compare them to typical Hi-C libraries. The spatial information exploited by proximity ligation is largely intact in FFPE specimens (**Figure 1C**). Each library was assessed for PCR duplication rate, unmapped rate, low map quality, and the insert distribution rate of high quality read pairs (**Supplemental Table S2**). PCR duplication rate is used to estimate library complexity. The insert distribution rates are used to assay the quality of the Fix-C library. Fix-C libraries that contain a high percent of reads pairs mapping to an insert size of 0 to 1kb contain very few long-range linkages and are therefore of poor use for downstream applications. Fix-C libraries that are of good quality typically contain several percent of reads in insert distribution bins greater than 1kb.

The basis of typical Fix- C analysis assumes that linked DNA sequencing read pairs have close spatial proximity in the 3-dimensional DNA polymer. Genomes harboring structural variation will produce sequencing read pair data with an accumulation of proximity contact between regions of the genome distant in proximity in the reference genome (**Figure 1D**) or on different chromosomes. In this approach, the read pair density is compared to what would be expected under the assumption that the genome is not rearranged. This signal produces dense clustering with clear discrete boundaries, which differ from the background signal of random chromosomal 3-dimensional conformations. The inference from this observation is that the genome in question has undergone a translocation to bring two disparate regions of the genome

together. This observation forms the basis for our approach to reliably identify structural variation and genome rearrangements from FFPE proximity ligation data.

Proximity ligation data represent a wealth of information that can be used for genome assembly, genome scaffolding, and studying how the genome is spatially organized. We were curious however to determine whether proximity ligation data derived from clinical FFPE samples can be used to detect structural rearrangements, such as gene fusion events in cancers. Fix-C was therefore performed on a panel of 15 FFPE tumor samples (**Table 1**) that had been previously characterized for gene fusions events via FISH and/or RNAseq. After library quality control and complexity estimation, each library was sequenced deeply enough to capture its estimated number of unique molecules. After aligning the read pairs to the human reference genome, the insert distribution of reads mapping to long range signals was determined; quantified here as the percent of total read pairs that span an insert distribution between 100Kb and 1Mb (**Table 1**).

To identify whether the gene fusion events previously detected by FISH could be visualized, linkage density plots at the FISH-confirmed loci were created for each FFPE sample (**Supplemental Figure S1**). **Figure 2A** demonstrates typical Fix-C translocation signal with dense ligation proximity contacts between the known rearranged gene regions with a discrete boundary. The complementary non-rearranged regions display only low-level background signal between the same loci (eg, sample 5 *MYO5C-ROS1*, sample 9 *ETV6-NTRK3*, and sample 8 *EML4-ALK*). Note that sample 9 tested negative for a *ROS1* fusion via FISH but was orthogonally confirmed as *MYO5C-ROS1* fusion positive via Fix-C and RNAseq. Across the clinical specimen cohort, 10 of the 15 Fix-C samples contained FISH confirmed fusions, two samples screened negative for *ROS1* FISH fusions (sample 9 was a false negative FISH result),

two samples were not FISH tested, and one sample tested positive for a *STAT6* fusion via IHC but missed by Fix-C (sample 7). The IHC and RNAseq called *STAT6-NAB2* fusion for sample 7 could not be assessed due to the extremely close proximity of the two genes to each other on chromosome 12. Of the two samples not FISH tested, one sample (sample 10) had a fusion detected by RNAseq but in-depth analysis of the Fix-C data show no proximity ligation read support for this event. Of the 10 FISH confirmed fusions clinical specimens a 90% concordance rate was obtained using the Fix-C approach, and highlighted true positive fusions missed by FISH.

In addition to targeted fusion detection (**Supplemental Table S3**), the Fix-C approach allows for unbiased discovery of novel global genomic rearrangements. **Figure 2B** demonstrates one such instance in a single clinical sample. Subpanel 4 highlights a FISH-confirmed *MYB*+ gene fusion event. Previously uncharacterized complex rearrangement events are seen within chromosome 3, between chromosomes 3 and 6, and between chromosomes 3 and 14.

In addition to uniform, hypothesis-free, whole-genome detection of genomic rearrangements, Fix-C data can also be used to describe the three-dimensional architecture of the genome from FFPE samples. Recent work analyzing Hi-C data has shown that chromosomes in living cells are organized into regional globules known as topologically associated domains (TADs)[15]. TADs are fundamental units of gene expression regulation[16], are evolutionarily conserved[17], and have boundaries that are often established by the insulator CTCF and cohesion[18]. Importantly, it was recently shown that some genomic rearrangements that lead to cancer and other maladies do so through TAD re-organization rather than by effecting genes *per se*[19]. One paradigm for this effect is known as enhancer hijacking wherein a genomic rearrangement leads to a TAD reorganization[20]. When this reorganization places an enhancer in a

new or different TAD, it can drive expression of genes not usually under its control. TADs are found within proximity ligation data by identifying regions of abundance of inter-region contacts and a lack of contacts with adjacent regions. Fix-C data reliably capture the regional signal that describes TAD organization within our FFPE samples, recapitulating the signal seen in typical Hi-C data (**Figure 2C**).

Discussion

This study describes an analytical method called Fix-C that couples the genome scale structural resolution of Hi-C in a workflow for FFPE tissue analysis that is compatible with high-throughput short-read sequencing platforms. Critically, this approach compares favorably across a broad range of cancer types to current clinical gold-standard methods of structural variation detection such as FISH, and emerging orthogonal methods such as targeted RNA sequencing panel. Additionally, the study shows that Fix-C has the ability to characterize novel complex multi-locus structural variation in tumor tissue that is missed by other approaches. Lastly, the study describes how this method can be leveraged to obtain high-level cellular spatial organization such as topologically-associated domains (TADs).

Further studies will be required to understand the lower limit of tumor purity for sensitive structural variation detection and whether this approach can be applied to small populations of cells or at the single-cell level. Recent studies characterizing tumor cell-free DNA (cfDNA) circulating as nucleosomes or chromatosomes[21], suggest this approach may hold promise for gene fusion detection and tissue-of-origin analysis in peripheral blood 'liquid biopsy' specimens.

The results suggest a deeper layer of cellular structural organization information is obtainable from archival FFPE tumor specimens typically used for pathological diagnosis,

prognosis, and prediction testing. With the growing body of literature implicating specific gene rearrangement events with targeted therapies, or serving as diagnostic biomarkers, it will be crucial to use robust genome-scale resolution methods such as Fix-C to tailor patient clinical management and explore novel biological structural phenomena.

In addition to the benefits of this approach, there are several current limitations. For example, structural rearrangements whose breakpoints are close together along the reference genome are necessarily more difficult to detect. The underlying signal of Fix-C is the number of proximity data points between any two regions of the genome. Genomic rearrangements induce an excess of proximity pairs between regions of the genome that ordinarily do not have them. However, if the breakpoints are already close together it may be difficult to detect the excess proximity events from the background of some expected proximity events. Further work will be necessary to characterize this limit of detection and to establish guidelines for necessary sequencing depth. Additionally, a 5kb bin resolution window is used for Fix-C analysis to scan the genome for rearrangement events, thus limiting exact nucleotide level breakpoint resolution—especially, within repetitive regions of the genome.

In summary, by leveraging a perceived limitation of archival tissue, we have developed a new method and data type for characterizing formalin-fixed, paraffin-embedded tumor tissue. Overall, our combined experimental and computational assay adds an additional approach to identify genomic spatial organization and rearrangements across a range of cancer types and tumor purity that may be clinically actionable and provides important insight into novel tumor biology and cancer dysfunction.

Conclusions

Tumor malignancies are often driven by gene fusion events or other genomic structural variations. A common practice for clinical solid tumor tissue is to undergo FFPE processing prior to pathology testing. However, the chemical modifications introduced to DNA during the formalin cross-linking and the dehydration processes results in highly fragmented, low molecular weight DNA molecules; making the detection of genomic structural variations by molecular methods, including DNA sequencing, difficult. Fix-C takes advantage of the formalin fixing process and native chromatin in FFPE tissues in order to producing chimeric read-pairs that spans large genomic distances through proximity ligation techniques. The result of Fix-C is data, produced on a short-read sequencer, which can detect global genomic structural variation events and chromatin conformation information from FFPE tissue.

Acknowledgements

C.J.T. performed the Fix-C experiments. N.H.P., S.S., and J.O.G. performed the computational analyses.

References

1. Blow N. Tissue preparation: Tissue issues. *Nature*. 2007;448(7156):959-963.

2. Wang F, Wang L, Briggs C, Sicinska E, Gaston SM, Mamon H, Kulke MH, Zamponi R, Loda M, Maher E, Ogino S, Fuchs CS, Li J, Hader C, Makrigiorgos GM. DNA degradation test predicts success in whole-genome amplification from diverse clinical samples. *J Mol Diagn*. 2007;9(4):441-451.

3. Srinivasan M, Sedmak D, Jewell S. Effect of fixatives and tissue processing on the content and integrity of nucleic acids. *Am J Pathol*. 2002;161(6):1961-1971.

4. Wang Q, Xia J, Jia P, Pao W, Zhao Z. Application of next generation sequencing to human gene fusion detection: computational tools, features and perspectives. *Briefings in Bioinformatics*. 2013;14(4):506-519.

5. Lawson ARJ, Hindley GFL, Forshew T, Tatevossian RG, Jamie GA, Kelly GP, Neale GA, Ma J, Jones TA, Ellison DW, Sheer D. RAF gene fusion breakpoints in pediatric brain tumors are characterized by significant enrichment of sequence microhomology. *Genome Research*. 2011;21(4):505-514.

6. Bonev B, Cavalli G. Organization and function of the 3D genome. *Nat Rev Genet*. 2016;17(11):661-678.

7. Burton JN, Adey A, Patwardhan RP, Qiu R, Kitzman JO, Shendure J. Chromosome-scale scaffolding of de novo genome assemblies based on chromatin interactions. *Nat Biotechnol*. 2013;31(12):1119-1125.

8. Selvaraj S, R Dixon J, Bansal V, Ren B. Whole-genome haplotype reconstruction using proximity-ligation and shotgun sequencing. *Nat Biotechnol*. 2013;31(12):1111-1118.

9. Putnam NH, O'Connell BL, Stites JC, Rice BJ, Blanchette M, Calef R, Troll CJ, Fields A, Hartley PD, Sugnet CW, Haussler D, Rokhsar DS, Green RE. Chromosome-scale shotgun assembly using an in vitro method for long-range linkage. *Genome Research*. 2016;26(3):342-350.

10. Zaharia M, Bolosky WJ, Curtis K, Fox A, Patterson D, Shenker S, Stoica I, Karp RM, Sittler T. Faster and More Accurate Sequence Alignment with SNAP. *arXiv*:1111.5572 [cs.DS]

11. Bailey JA, Gu Z, Clark RA, Reinert K, Samonte RV, Schwartz S, Adams MD, Myers EW, Li PW, Eichler EE. Recent segmental duplications in the human genome. *Science*. 2002;297(5583):1003-1007..

12. Wang K, Li M, Hakonarson H. ANNOVAR: functional annotation of genetic variants from high-throughput sequencing data. *Nucleic Acids Res*. 2010;38(16):e164-e164.

13. Nybakken GE, Bala R, Gratzinger D, Jones CD, Zehnder JL, Bangs CD, Cherry A, Warnke RA, Natkunam Y. Isolated Follicles Enriched for Centroblasts and Lacking t(14;18)/BCL2 in Lymphoid Tissue: Diagnostic and Clinical Implications. Pagano JS, ed. *PLoS ONE*. 2016;11(3):e0151735. doi:10.1371/journal.pone.0151735.

14. Schmitt AD, Hu M, Ren B. Genome-wide mapping and analysis of chromosome architecture. *Nat Rev Mol Cell Biol*. 2016;17(12):743-755.

15. Dixon JR, Selvaraj S, Yue F, Kim A, Li Y, Shen Y, Hu M, Liu JS, Ren B. Topological domains in mammalian genomes identified by analysis of chromatin interactions. *Nature*. 2012;485(7398):376-380.

16. Nora EP, Lajoie BR, Schulz EG, Giorgetti L, Okamoto I, Servant N, Piolot T, van Berkum NL, Meisig J, Sedat J, Gribnau J, Barillot E, Bluthgen N, Dekker J, Heard E. Spatial partitioning of the regulatory landscape of the X-inactivation centre. *Nature*. 2012;485(7398):381-385.

17. Dixon JR, Jung I, Selvaraj S, Shen Y, Antosiewicz-Bourget JE, Lee AY, Ye Z, Kim A, Rajagopal N, Xie W, Diao Y, Liang J, Zhao H, Lobanenjov VV, Ecker JR, Thomson J, Ren B. Chromatin architecture reorganization during stem cell differentiation. *Nature*. 2015;518(7539):331-336.

18. Fudenberg G, Imakaev M, Lu C, Goloborodko A, Abdennur N, Mirny LA. Formation of Chromosomal Domains by Loop Extrusion. *Cell Rep*. 2016;15(9):2038-2049.

19. Valton A-L, Dekker J. TAD disruption as oncogenic driver. *Curr Opin Genet Dev*. 2016;36:34-40.

20. Lupiáñez DG, Spielmann M, Mundlos S. Breaking TADs: How Alterations of Chromatin Domains Result in Disease. *Trends Genet*. 2016;32(4):225-237.

21. Snyder MW, Kircher M, Hill AJ, Daza RM, Shendure J. Cell-free DNA Comprises an In Vivo Nucleosome Footprint that Informs Its Tissues-Of-Origin. *Cell*. 2016;164(1-2):57-68.

Figure Legends

Figure 1. Fix-C method and data-types. **A:** Fix-C experimental methodology. Cross-linked (red lines) DNA-histone complexes (black lines and blue circles, respectively) are extracted from formalin-fixed, paraffin-embedded (FFPE) samples. The DNA fragments are digested (black lines with overhangs) and biotinylated (green circles)—serving as a marker for subsequent enrichment. The biotinylated DNA fragments are subsequently re-ligated in conditions that promote ligation of neighboring DNA chromatin fragments in close physical proximity (red asterisks). Following crosslink reversal, DNA shearing, and biotin capture on streptavidin beads, standard Hi-C–like high-throughput sequencing libraries are generated and the proximity of the ligated DNA is then measured by DNA sequencing (grey arrows). **B:** DNA fragment distribution (black area) from high molecular weight non-fixed tissue (middle) and degraded FFPE tissue DNA (right). The lower bound 100bp fragment size marker is denoted as a green line in each sample. **C:** Read pair separation in FFPE proximity ligation. Each read in a pair is mapped to the reference human genome. Shown here is a histogram of the frequencies of increasing distances spanned between reads in a pair. Reads of increasingly farther distance are less likely to be observed, yet many read pairs span hundreds or thousands of kilobases. **D:** Example Fix-C linkage density plot visualization of a translocation. Each pixel represents an interaction (ie, proximity ligation read pair mapping) between randomly ligated DNA fragments. Read pair associations between known adjacent neighboring sequences occur at the base of the triangle, whereas those between distal sequences in cis or on other chromosomes occur 'off-the-diagonal'. A genomic translocation event between Locus A and Locus B is inferred due to the high concentration of proximity ligation read pair mapping (red circle).

Figure 2. Fix-C detection of known and novel genomic rearrangements in clinical samples.

A: *ALK* (sample 5) and *ETV6* (sample 8) gene fusion events are detected by Fix-C. A *ROS1* fusion is detected from a sample with a false negative *ROS1* fluorescence *in situ* hybridization (FISH) result by Fix-C (sample 9). Samples known to harbor genomic rearrangements show strong signal of proximity between the examined loci whereas others act as controls, displaying only background signal between the same loci. **B:** Fix-C discovery of undetected global genomic rearrangements in a single clinical sample. FISH-confirmed MYB^{+} (subpanel 4) gene fusion events are detected by Fix-C. Novel complex genome rearrangement events in a single sample detected within chromosome 3 (subpanel 1), between chromosomes 3 and 6 (subpanel 2), and between chromosomes 3 and 14 (subpanel 3). **C:** An 18Mbp locus on chromosome 2 demonstrating the characteristic pattern of increased interactions within topologically associated domains (TADs). TADs display as triangles of high contact frequency within TADs. The bottom panel shows contact frequency within a typical Hi-C sample. Panels above show the same TAD organization across this region in Fix-C samples.

Table 1. Summary of samples tested, FISH/Fix-C/RNAseq fusion detection, and Fix-C sequencing metrics.

General Information			Fusion Calls - Confirmed	Fusion Calls - FISH Concordance		Fix-C Sequencing Metrics	
Sample Number	**Histology**	**Tumor Percentage**	**FISH**	**Fix-C**	**RNAseq**	**PCR Duplicate Rate**	**Reads Mapping to 100kb-1Mb Insert Size**
1	Lung adenocarcinoma	20	ALK+	NEG	NEG	2.94%	0.61%
2	Adenoid cystic carcinoma	50	MYB+	EWSR1-MYB	EWSR1-MYB	0.16%	8.00%
3	Round cell liposarcoma	90	FUS+	DDIT3-FUS	DDIT3-FUS	6.35%	5.45%
4	Extraskeletal myxoid chondrosarcoma	60	EWSR1+	EWSR1-NR4A3	EWSR1-NR4A3	2.77%	7.80%
5	Papillary thyroid carcinoma	90	--	EML4-ALK	EML4-ALK	0.19%	7.84%
6	Synovial sarcoma	90	SS18+	PAOX-SS18 SS18-SSX2B	SS18-SSX2	0.15%	1.93%
7	Solitary fibrous tumor, malignant	80	STAT6+ (IHC)	NEG	NAB2-STAT6	0.35%	9.53%
8	Mammary analog secretory carcinoma	30	ETV6+	ETV6-NTRK3	NTRK3-ETV6	1.43%	3.64%
9	Lung adenocarcinoma	50	NEG (ROS1 Tested)	MYO5C-ROS1	MYO5C-ROS1	0.68%	3.53%

10	Lung adenocarcinoma	60	NEG (ROS1 Tested)	NEG	KIF5B-RET	1.31%	6.56%
11	Angiomatoid fibrous histiocytoma	30	EWSR1+	EWSR1-CREB1	EWSR1-CREB1	0.43%	2.66%
12	Inflammatory myofibroblastic tumor	20	ALK+	CLTC-ALK	CLTC-ALK	0.11%	8.47%
13	Adenoid cystic carcinoma	80	MYB+	MYB-EWSR1	MYB-EWSR1	0.36%	8.03%
14	Synovial sarcoma	80	SS18+	SS18-SSX2B	SS18-SSX2	0.64%	5.50%
15	Normal spleen	0	--	NEG	--	0.07%	7.56%

'--' denotes samples without testing data. 'NEG' denotes samples where testing was performed and the results were negative.

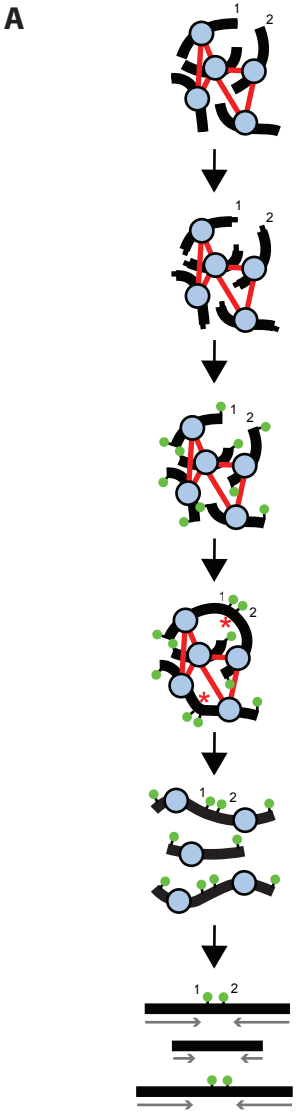

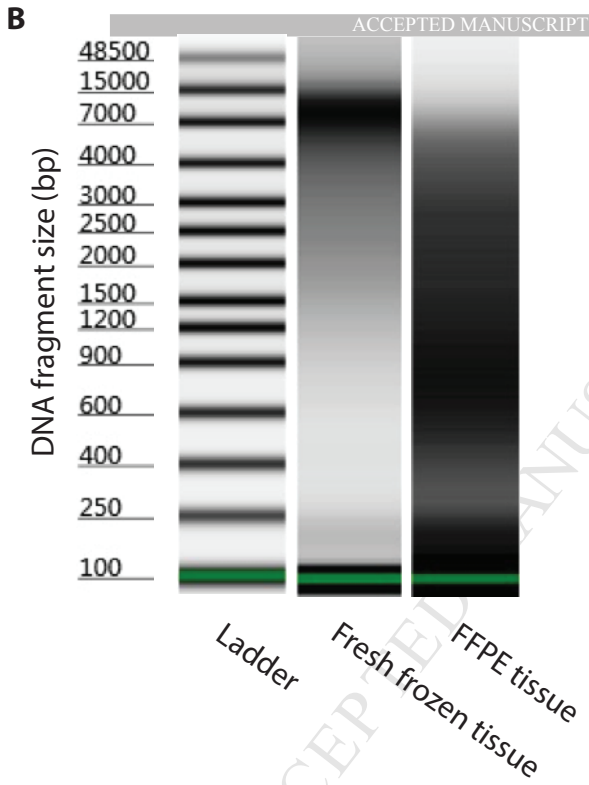

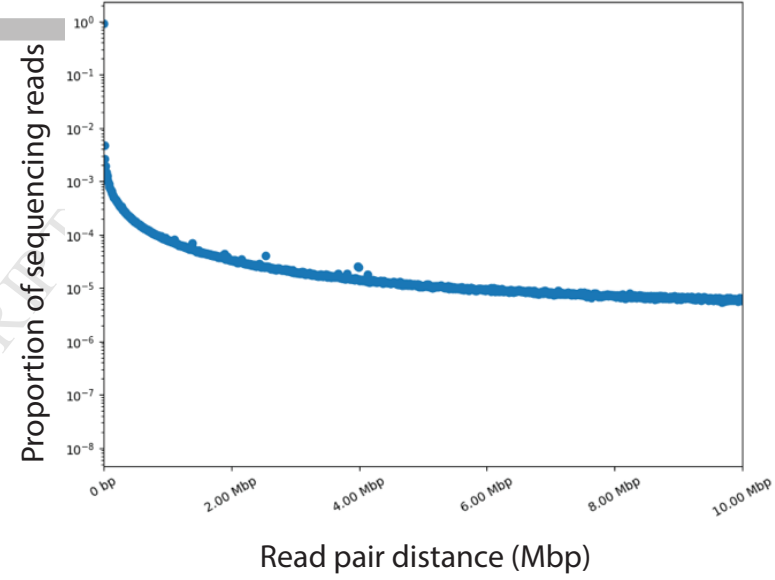

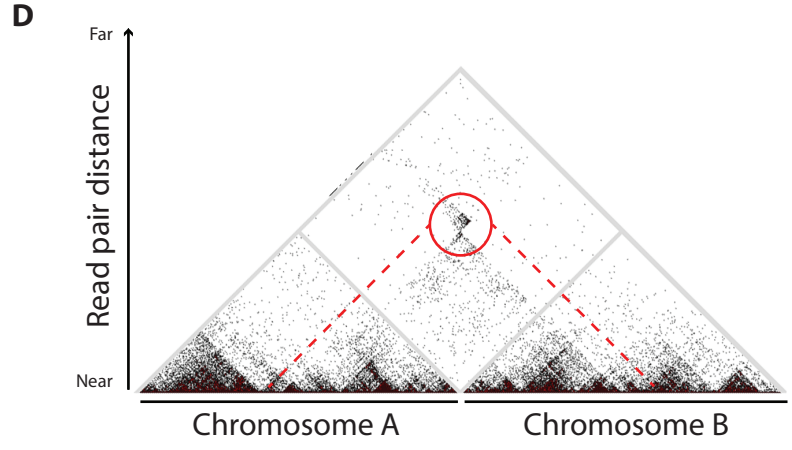

A

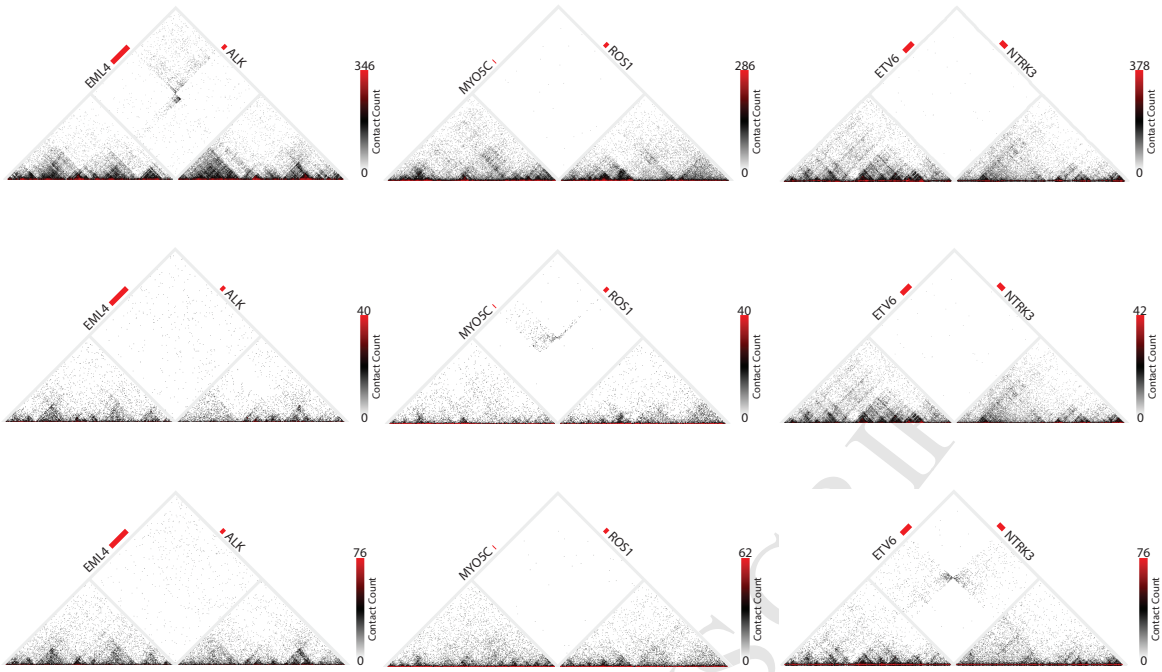

B

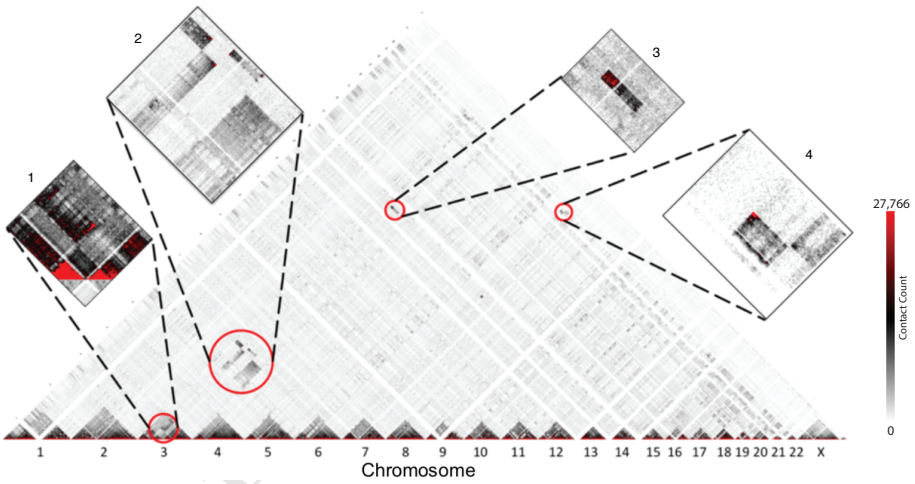

C